

The First Principles Calculations of Pt or Au Doping on Improving the Detection of CO by ZnO Using Density Functional Theory

Micheal Mage Dorin Zalinda¹, Rabiatul Adawiyah Rosli¹, Muhammad Ashraff Hamdan¹, Mohamad Syafie Mahmood¹, Mohamad Fariz Mohamad Taib², Nur Hafiz Hussin^{1*}

¹Faculty of Applied Sciences, Universiti Teknologi MARA, 26400 Jengka, Pahang, Malaysia

²Faculty of Applied Sciences, Universiti Teknologi MARA, 40450 Shah Alam, Selangor, Malaysia

*Corresponding Author's E-mail: hafizhussin@uitm.edu.my

Received: 06 February 2024

Accepted: 02 July 2024

Online First: 01 September 2024

ABSTRACT

ZnO doped with Pt or Au (Pt/Au-ZnO) exhibits strong gas response at room temperature, making it a promising gas sensing material. Since carbon monoxide (CO) is one of the most hazardous gases in both daily work and life operations, it's critical to develop gas sensors with excellent stability, sensitivity, and selectivity for CO gas. The aim of this study is to investigate the structural and electronic properties of crystal ZnO using CASTEP calculation, and also to elucidate the effect of Pt/Au on ZnO as CO detection with validated functional exchange correlation GGA-PBE that implemented in CASTEP computer code. For each doped material, the composition was changed with 100% of Pt/Au and 0% of O, 80% of Pt/Au and 20% of O, 60% of Pt/Au and 40% of O, 40% of Pt/Au and 60% of O, and 20% of Pt/Au and 80% of O. The geometrical optimization and energy were calculated by GGA-PBE. It is believed that noble metal surface modification of metal oxide is the most practical and efficient way to enhance gas sensing. Because of their strong catalytic activity, noble metal nanoparticles have been demonstrated in multiple studies to enhance ZnO's sensing capabilities. Furthermore, by doping noble metals which are Pt and Au with ZnO, it provides the insight of developing gas sensors for CO detection by determining the formation energy and understanding the



energy band structure and the density of states.

Keywords: Carbon monoxide; Density Functional Theory; First Principles; Sensor; Zinc Oxide

INTRODUCTION

Carbon monoxide (CO), one of the most dangerous gases in daily life as well as company operations, is colourless, odorless, and highly hazardous. It typically results from incomplete fuel combustion at home and in exhaust emissions from vehicles [1]. Carbon monoxide is also one of the mixtures contained in wildfire smoke. In addition to posing a number of risks to human health and economic difficulties, wildfire smoke and pollutants can spread far from the actual site of the fire where pregnant women and middle-aged and older people with acute or chronic respiratory and cardiovascular disorders are the populations most at risk from exposure to wildfire smoke. In recent years, the CO has produced a large number of intoxication victims worldwide. For instance, the General Directorate of Civil Protection in Algeria reported 134 deaths and over 2 928 victims of intoxication in the course of 2017. 3 354 intoxication victims were made by the CO in France in 2017 [2].

It is important to develop gas sensors with excellent carbon monoxide (CO) gas selectivity, sensitivity, and stability [3]. This is because environmental pollution and workplace safety are both major problems. Since its inception in 1962, the metal oxide semiconductor (MOS) gas sensor has undergone a great deal of development. It is one of the gas sensors that is most frequently used nowadays on a global scale. In comparison to other gas sensors, MOS gas sensors are more sensitive, less expensive, respond quicker, and last longer. A common material for high-sensitivity CO detection is ZnO, a typical n-type MOS semiconductor [1]. The development of affordable, trustworthy, and efficient poisonous gas sensors has recently sparked a lot of interest on a variety of levels, from industrial to medical applications [4].

The most effective and convenient method to improve gas sensing is thought to be noble metal surface modification of metal oxide. Noble

metal nanoparticles have been shown in numerous studies to improve ZnO's sensing capabilities due to their potent catalytic activity [5]. Due to its advanced properties, binary metal oxides like ZnO have been exploited as sensitive materials ever since the resistive gas sensor was discovered [6]. Gas sensors made of ZnO are generating a lot of interest since they nearly perfectly meet the criteria for the ideal sensor [7].

Understanding chemical reactivity, the structure-activity relationship, and interfacial chemical interactions are all made possible by first-principles calculations. First principles calculations, particularly via the density functional theory (DFT), have been widely used for the exploration of interfacial properties in recent years due to the huge expansion of high-performance computing (HPC) equipment, computational techniques, and software packages [8]. It is well known that density functional theory (DFT) is a promising and practical computational approach to precisely study the electrical structure of molecular systems [9]. Density functional theory approaches are the most popular and widely used theoretical techniques for computing electronic structure [10]. In this study, all theoretical calculations are based on first-principles calculations in Materials Studio and the CASTEP module completed model development, optimization, and parameter calculation. The calculation included geometrical optimization calculation in order to obtain accurate and reliable information about the structures and properties of Pt/Au-ZnO. Furthermore, the energy is also being calculated for the purpose of determining the band gap, density of state, and formation energy. All these calculations were performed in every composition of Au-ZnO and Pt-ZnO (100%, 80%, 60%, 40%, 20%).

METHODOLOGY

Structure Modelling of Pt/Au-ZnO

The structure of ZnO as indicated at Figure 1(a) was directly imported from the Material Studio CASTEP. The structure of ZnO after doped with Pt/Au was indicated at Figure 1(b).

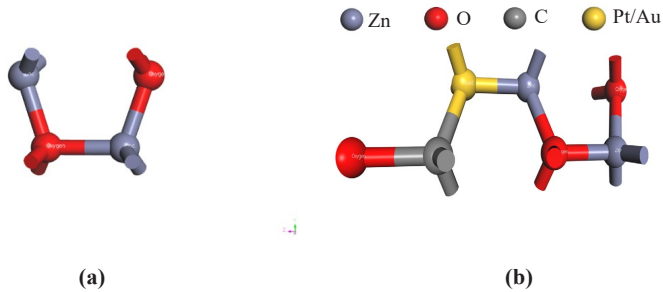


Figure 1: (a) Structure of ZnO, (b) Structure of Pt/Au-ZnO

Calculation

First principles calculations based on the density functional theory (DFT) are performed using Material Studio 7.0 from Accelrys Software Inc. In this research, the structural and electronic properties of ZnO and the effect of different concentrations Pt/Au ZnO investigated using a fully implemented computational method. The MS Visualiser was used in structure building for pure ZnO and Pt/Au doped ZnO. To address the exchange-correlation effect, the methods would be used: generalised gradient approximation (GGA) utilising the Perdew-Burke-Ernzerhof (PBE) function with pseudopotential plane wave method. The PBE functional is well known for its ability to predict structural characteristics and total energy with a reasonable degree of precision while retaining computational efficiency. PBE was used to ensure that we could run large calculations without incurring prohibitive computational expenses, given the available computer resources. Convergence tests were first carried out first with the convergence of energy change per atom $<5 \times 10^{-6}$ eV, residual force <0.01 eV/Å, stress <0.02 GPa and displacement of atoms <0.0005 Å [11]. For geometrical optimization, the structural analysis included the population analysis of Pt/Au doped ZnO, meanwhile for energy calculation, the structural analysis included the band structure and density of states.

Analysis

The structure of the materials that already undergo both geometry Optimization and energy calculation was used in analysis to calculate the formation energy for every composition. In this part, the band structure was analysed to obtain the band gap. Moreover, the partial density of state was analysed to determine which orbitals were dominated in the highest valence band, and in the lowest conduction band.

RESULTS AND DISCUSSION

Structural properties of Pt/Au-ZnO

In this work, the structure selected for calculation was a ZnO crystal, which was composed of a 1 x 1 x 1 supercell structure. Figure 1 (b) shows the structure of Pt/Au doped with ZnO with a different composition of Pt/Au which is 100% of Pt/Au and 0% of O, 80% of Pt/Au and 20% of O, 60% of Pt/Au and 40% of O, 40% of Pt/Au and 60% of O, and 20% of Pt/Au and 80% of O. This paper's theoretical computations were all first-principles calculations performed in Materials Studio (MS). The CASTEP module finished the computation of energy, optimization, and model building. The structure was optimised using the generalised gradient approximation developed by Perdew-Burke-Ernzerhof (GGA-PBE) from the approximated geometry optimization functional to obtain accurate and reliable information about the structure and properties of the material. After performing the geometrical optimization calculation, the energy has been calculated in order to determine the band gap, formation energy, and the density of state. Table 1 until Table 5 summarises the energy of each component and their number of atoms, final energy, and formation energy for each composition for Au-ZnO. For Pt-ZnO, the energy of each component and their number of atoms, final energy, and formation energy for each composition are summarised in Table 6 until Table 10.

The number of atoms for each element is based on Figure 1(b) where there are 2 atoms for Zinc, 1 atom for Carbon, 3 atoms for Oxygen, and 1 atom for Platinum/Gold. As the composition changes, the number of atoms also changes. When the composition was 0.8Au/Pt and 0.2O (Table 2, Table

7), the number of atoms for Au/Pt was decreased to 0.8 whereas the number of atoms for O was increased to 3.20. As the value of the composition decreases, the number of atoms for O will increase whereas the number of atoms for Pt/Au will decrease.

From these tables, it can be seen that all of the formation energy is negative except for Au-ZnO with 0.2Au composition. Negative formation energy means that the displacement process is exothermic, while on the other hand, positive formation energy means that the displacement process is endothermic [1]. For positive formation energy (endothermic), energy from their environment is absorbed by endothermic processes. This means that in order for doping or displacement to take place, energy needs to be provided to the system, just like in any other formation process. It suggests that an external energy source is required to induce the dopant's incorporation into the crystal lattice and that the doped material is less stable than the undoped material. On the other hand, for negative formation energy (exothermic), energy is released into the environment during exothermic processes [1]. This implies that energy is released throughout the displacement or doping process, whether it be in the context of doping or another formation process. It suggests that the doped material is more stable than the undoped material and that heat is released during the spontaneous dopant incorporation into the crystal lattice. Researchers have also recently researched using Fe as a doping element. In this way, utilising the spin-coating technique, researcher created a gas sensor by depositing Fe-doped ZnO thin films over a conducting glass. Compared to the undoped ZnO, this device exhibited notably higher CO gas detection sensitivity, good gas responsiveness, and better stability [12]. In this calculation, the bulk phases were taken as reference systems for its individual components, Au/Pt, C, Zn, and O. The formation energy of these bulk from Au/Pt, C, Zn, and O bulk were calculated using the formula in Eq. (1):

$$E_{formation} = E_{total} - \frac{E_{Zn}}{n} - \frac{E_C}{n} - \frac{E_O}{n} - \frac{E_{Au/Pt}}{n} \quad (1)$$

where n is the number of atoms in the Au/Pt, C, Zn, and O bulk unit cells, respectively.

Table 1: Au-ZnO with 1.0Au and 0.0O composition

Components	Zinc, Zn	Carbon, C	Oxygen, O	Gold, Au
Energy, eV	-1708.0392	-145.8231	-429.5309	-910.5826
No. of atom	2	1	3	1
Final energy, eV	-5796.7097			
Formation energy, eV	-3743.1074			

Table 2: Au-ZnO with 0.8Au and 0.2O composition

Components	Zinc, Zn	Carbon, C	Oxygen, O	Gold, Au
Energy, eV	-1708.0392	-145.8231	-429.5309	-910.5826
No. of atom	2	1	3.2	0.8
Final energy, eV	-5727.7933			
Formation energy, eV	-3455.4939			

Table 3: Au-ZnO with 0.6Au and 0.4O composition

Components	Zinc, Zn	Carbon, C	Oxygen, O	Gold, Au
Energy, eV	-1708.0392	-145.8231	-429.5309	-910.5826
No. of atom	2	1	3.4	0.6
Final energy, eV	-5668.9213			
Formation energy, eV	-3025.1083			

Table 4: Au-ZnO with 0.4Au and 0.6O composition

Components	Zinc, Zn	Carbon, C	Oxygen, O	Gold, Au
Energy, eV	-1708.0392	-145.8231	-429.5309	-910.5826
No. of atom	2	1	3.6	0.4
Final energy, eV	-5599.5353			
Formation energy, eV	-2203.9220			

Table 5: Au-ZnO with 0.2Au and 0.8O composition

Components	Zinc, Zn	Carbon, C	Oxygen, O	Gold, Au
Energy, eV	-1708.0392	-145.8231	-429.5309	-910.5826
No. of atom	2	1	3.8	0.2
Final energy, eV	-5454.2109			
Formation energy, eV	211.5793			

Table 6: Pt-ZnO with 1.0Pt and 0.0O composition

Components	Zinc, Zn	Carbon, C	Oxygen, O	Gold, Au
Energy, eV	-1708.0392	-145.8231	-429.5309	-712.0013
No. of atom	2	1	3	1
Final energy, eV	-5602.4743			
Formation energy, eV	-3747.4534			

Table 7: Pt-ZnO with 0.8APt and 0.2O composition

Components	Zinc, Zn	Carbon, C	Oxygen, O	Gold, Au
Energy, eV	-1708.0392	-145.8231	-429.5309	-712.0013
No. of atom	2	1	3.2	0.8
Final energy, eV	-5559.4643			
Formation energy, eV	-3535.3916			

Table 8: Pt-ZnO with 0.6Pt and 0.4O composition

Components	Zinc, Zn	Carbon, C	Oxygen, O	Gold, Au
Energy, eV	-1708.0392	-145.8231	-429.5309	-712.0013
No. of atom	2	1	3.4	0.6
Final energy, eV	-5528.7775			
Formation energy, eV	-3215.9334			

Table 9: Pt-ZnO with 0.4Pt and 0.6O composition

Components	Zinc, Zn	Carbon, C	Oxygen, O	Gold, Au
Energy, eV	-1708.1199	-145.8263	-429.5634	-712.0093
No. of atom	2	1	3.6	0.4
Final energy, eV	-5489.7217			
Formation energy, eV	-2590.4890			

Table 10: Pt-ZnO with 0.2Pt and 0.8O composition

Components	Zinc, Zn	Carbon, C	Oxygen, O	Gold, Au
Energy, eV	-1708.1199	-145.8263	-429.5634	-712.0093
No. of atom	2	1	3.8	0.2
Final energy, eV	-5377.2422			
Formation energy, eV	-704.2664			

Figure 2 and Figure 3 shows the comparison of the formation energy between each composition of the materials. Based on these figures, it can be seen that the Au/Pt-ZnO (100% composition) are the lowest formation energies among the other compositions. The smaller the formation energy is, the more likely doping is to occur, and the more stable the resulting structure is [1]. Moreover, by comparing Pt-ZnO with Au-ZnO at 100% composition, it can be seen that Pt-ZnO is slightly higher than Au-ZnO where the formation energy for Pt-ZnO is -3747.4534 eV and -3743.1074 eV for Au-ZnO.

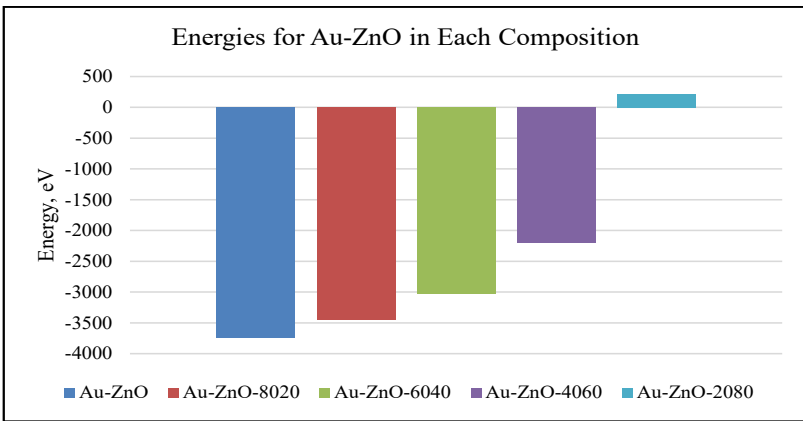


Figure 2: Graph for energies for Au-ZnO in different composition

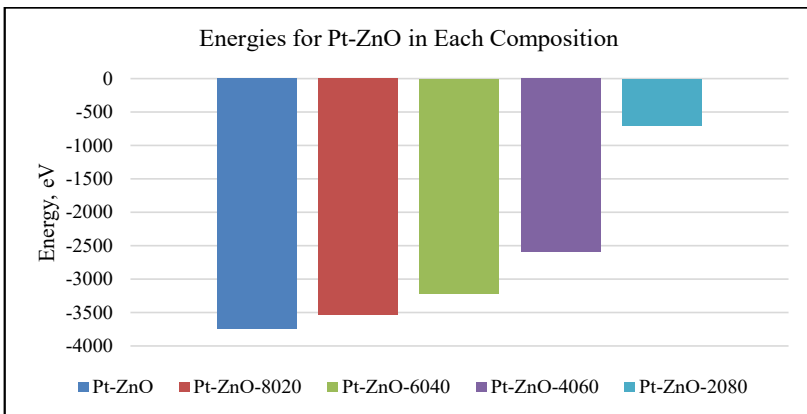


Figure 3: Graph for energies for Pt-ZnO in different composition

The stability of a specific crystal structure or chemical configuration is gauged by a material's formation energy. The formation energy of the dopant in doped materials used for sensors can reveal information about the chances of successful doping as well as how it affects the sensor's overall performance. A lower formation energy suggests a higher probability of stable configuration incorporation of the dopant into the host material. This suggests that the doped material is more likely to retain its structure over time and is energetically beneficial. Besides that, a lower formation energy for the doped configuration indicates a higher probability of the dopant remaining in the desired location within the material's crystal lattice. Because of the potential for a more consistent and predictable impact of the dopant's presence on the material's characteristics, this stability may result in enhanced sensor performance. In addition, a lower formation energy suggests that the dopant is less likely to diffuse or create vacancies in the material, which is essential for preserving the sensitivity and dependability of the sensor. Over time, the performance of the sensor may be deteriorated by unwanted diffusion or vacancy development.

Energy band structure

In Figure 4 and Figure 5, the calculated electronic band structures of Pt and Au doped with ZnO for each composition using GGA-PBE functional are illustrated for the energy ranges of -10 to 10 eV, respectively, along the direction of the high symmetry Brillouin zone (G-F-Q-Z-G). 0 eV is representing the Fermi level. Table 11 and Table 12 shows the band gap calculated after performing the energy calculation using CASTEP. Furthermore, the morphological, chemical, and electrical properties of the material - specifically, the band gap - are essential for improving the sensitivity of sensors [13].

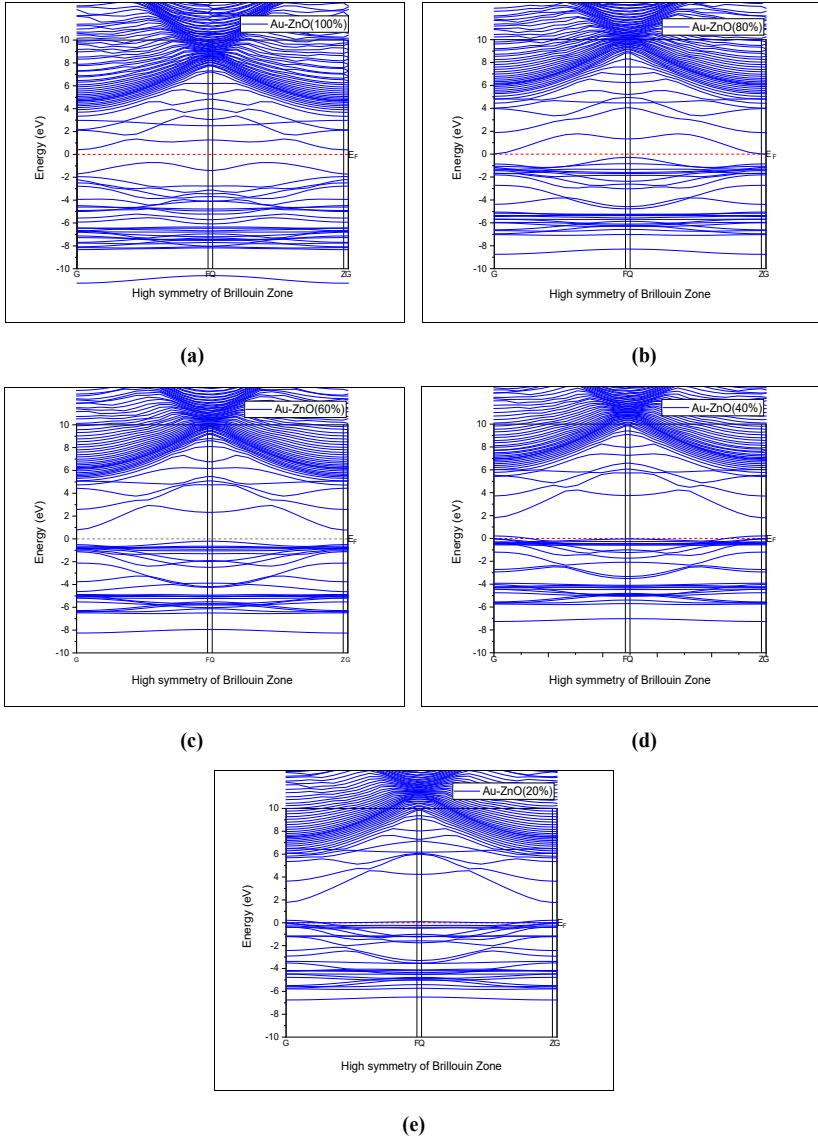


Figure 4: Energy band structure of (a) Au-ZnO(100%), (b) Au-ZnO(80%), (c) Au-ZnO(60%), (d) Au-ZnO(40%), (e) Au-ZnO(20%)

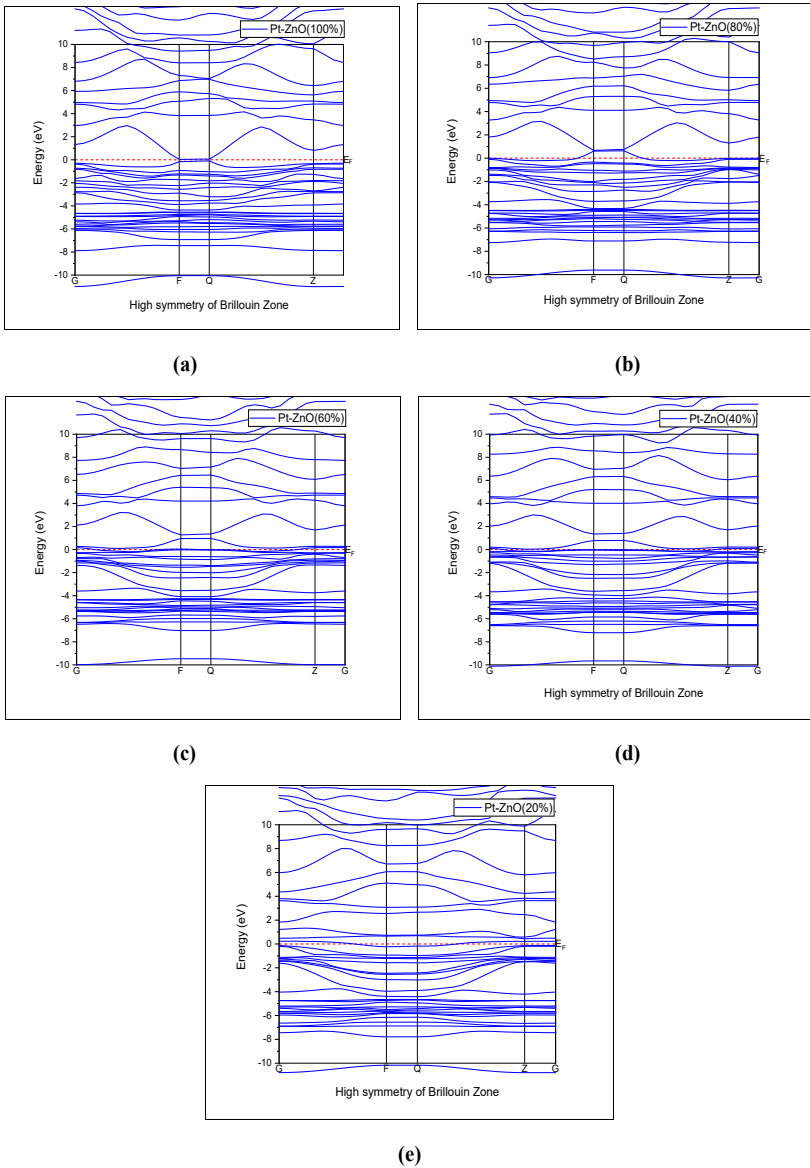


Figure 5: Energy band structure of (a) Pt-ZnO(100%), (b) Pt-ZnO(80%), (c) Pt-ZnO(60%), (d) Pt-ZnO(40%), (e) Pt-ZnO(20%)

From Table 11 and 12, it can be seen that the CASTEP only shows the value of band gap for 1.0Au, 0.0O, 0.8Au, 0.2O, 0.6Au, 0.4O, and 1.0Pt, 0.0O. Based on Figure 4 (a) (b) (c), and Figure 5 (a), the conduction band and valence band are not crossing the Fermi level. As a result, the software is automatically providing the band gap value (small gap at Fermi level). However, as can be seen in Figures 4 (d) (e) and Figure 5 (b) (c) (d) (e), the valence bands overlap the Fermi level, making it unable for the software to identify a gap in those conduction and valence bands. The valence band is the highest energy band that is fully occupied by electrons at absolute zero temperature. Electrons in this band are tightly bound to atoms. The next higher energy band, the conduction band, is empty at absolute zero. This band allows electrons to freely travel and contribute to electrical conduction. The energy level at which there is a 0.5 chance of detecting an electron at absolute zero is known as the Fermi level. It is a measurement of the maximum energy state that electrons can occupy at zero temperature. The minimum energy of the conduction band and the highest energy of the valence band coincide at the same momentum (k-point) in the Brillouin zone of a material having a direct band gap. Without changing their momentum, electrons can move with ease from the valence band to the conduction band. The straight band gap is the energy difference between the minimum of the conduction band and the maximum of the valence band. These transitions do not directly involve the Fermi level. On the other hand, the highest energy of the valence band and the minimum energy of the conduction band occur at separate k-points in a material having an indirect band gap. Transitioning electrons between the valence and conduction bands need momentum changes, which reduces the efficiency of the operation. The energy level where transitions from the valence band to the conduction band are most likely to occur is represented by the Fermi level, which makes it significant in indirect transitions. According to the previous research about ‘Adsorption studies on air pollutants using blue phosphorene nanosheet as a chemical sensor – DFT approach’, it states that, from overall, the observation strongly suggests that the main blue phosphorene nanosheet sensor (BPNS) is a promising sensor of NO and NO², even in the presence of dampness as the energy gap of 1.999 eV in pure BPNS demonstrate its structural stability [14]. Hence, the band gap for both materials which are Au-ZnO and Pt-ZnO with 100% of Pt/Au and 0% for O composition are good to be considered as stable for the sensor.

Table 11: Calculated band gap for Pt-ZnO

Materials	Composition	Band gap, eV
Au-ZnO	1.0Au, 0.0O	1.119
	0.8Au, 0.2O	0.301
	0.6Au, 0.4O	0.984
	0.4Au, 0.6O	0
	0.2Au, 0.8O	0

Table 12: Calculated band gap for Pt-ZnO

Materials	Composition	Band gap, eV
Pt-ZnO	1.0Pt, 0.0O	0.132
	0.8Pt, 0.2O	0
	0.6Pt, 0.4O	0
	0.4Pt, 0.6O	0
	0.2Pt, 0.8O	0

Partial density of state (PDOS)

In condensed matter physics and materials science, the Partial Density of States (PDOS) idea is used to investigate a material’s electrical structure more thoroughly. The Density of States (DOS) gives details on the energy-wise distribution of electronic states in a material. By separating the DOS into contributions from certain atomic orbitals or orbital groups, the PDOS goes one step farther in this regard. In this part, as Pt/Au-ZnO with 100% composition has the lowest formation energy among the others composition, hence, only their PDOS would be analysed.

Figure 6 shows the PDOS for Au-ZnO and its component elements, which also illustrates the distribution of electronic states at different levels of energy. Every sub-figure is focusing on a certain element: Figure 6(a) shows the PDOS of Au-ZnO, highlighting the contributions from Au and ZnO. Figure 6(b) presents the PDOS of gold, highlighting its 6s and 5d orbitals. Figure 6(c) shows the PDOS of zinc, showcasing its 4s and 3d orbitals. Figure 6(d) presents the PDOS of oxygen, showcasing its 2s and 2p orbitals. While PDOS of carbon is shown in Figure 6(e), indicating the presence of 2s and 2p orbitals.

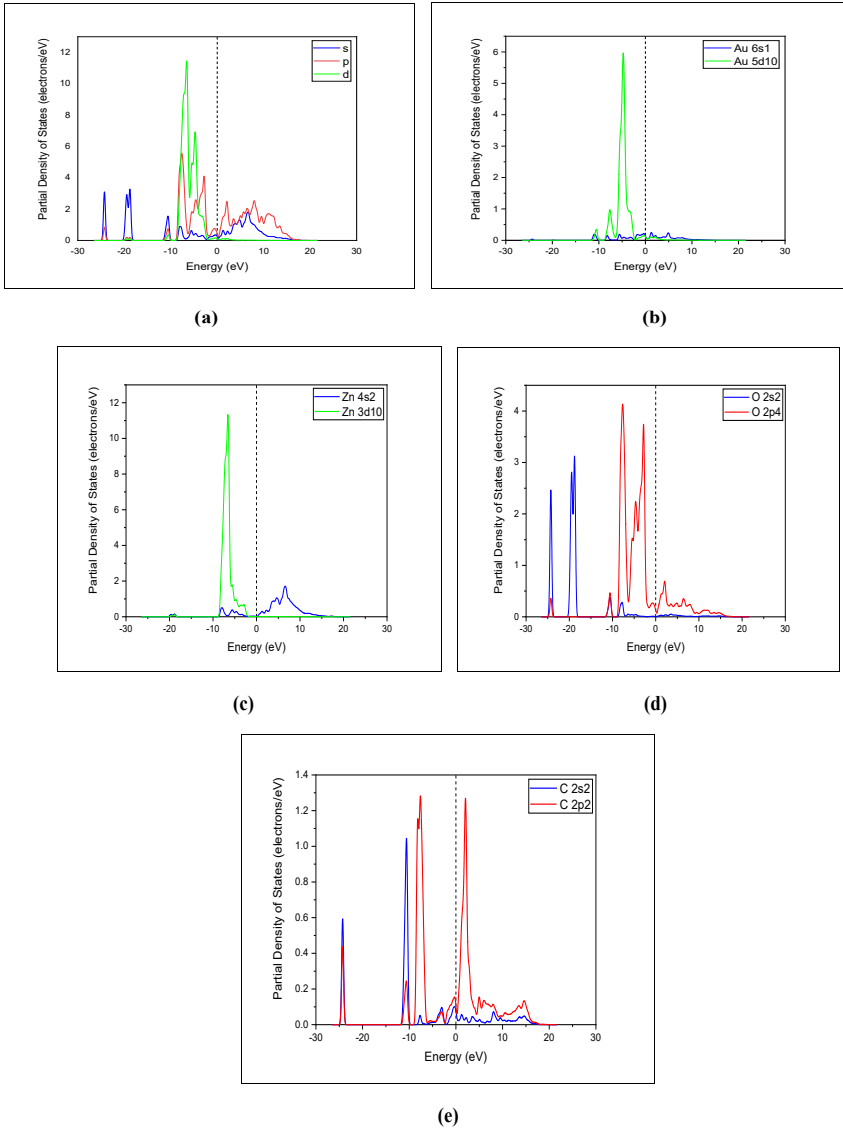


Figure 6: Partial Density of States (PDOS) of (a) Au-ZnO, (b) Au, (c) Zn, (d) O, (e) C

Similarly, the PDOS for Pt-ZnO and each of its components is shown in Figure 7: Figure 7(a) shows the PDOS of Pt-ZnO, highlighting the contributions from Pt and ZnO. Figure 7(b) presents the PDOS of platinum, highlighting its 6s and 5d orbitals. Figure 7(c) shows the PDOS of zinc, showcasing its 4s and 3d orbitals. Figure 7(d) presents the PDOS of oxygen, showcasing its 2s and 2p orbitals. While PDOS of carbon is shown in Figure 7(e), indicating the presence of 2s and 2p orbitals.

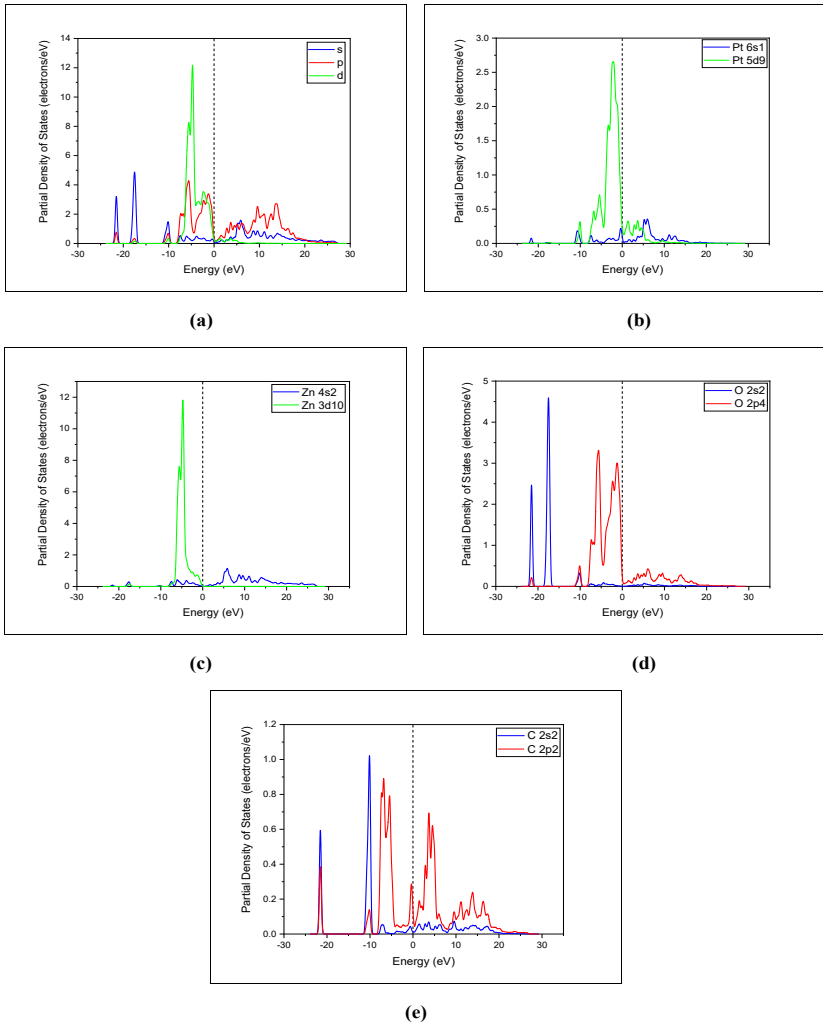


Figure 7: Partial Density of States (PDOS) of (a) Pt-ZnO, (b) Pt, (c) Zn, (d) O, (e) C

According to Figure 6, the electron Zn 3d¹⁰ orbital is dominating in the highest valence band of Au-ZnO. This means that the states responsible for the highest energy electrons in the valence band largely emerge from the Zn 3d¹⁰ orbitals. The Zn 2s² and O 2p⁴ states contribute to the lowest conduction band. On the other hand, according to Figure 7, the electron Zn 3d¹⁰ orbital contributes to the highest valence band of Pt-ZnO. In addition, the Zn 4s² and O 2p⁴ states contribute to the lowest conduction band.

The impact of doping on the material's electronic structure, which in turn affects its sensing properties, is the link between the Partial Density of States (PDOS) of doped materials and their use in sensors. Doping is the deliberate addition of impurities to a material in order to change some of its characteristics. The electron Zn 3d¹⁰ orbital contributes to the highest valence band implies that variations in Zn 3d¹⁰ state occupancy may be susceptible to outside influences. This sensitivity can be used in sensing applications where changes in the electrical structure of the sensor indicate changes in its surroundings. Various orbitals contribute to different bands; examples are Zn 3d¹⁰, Zn 4s², and O 2p⁴. Due to the particular orbitals involved, this may produce a sensor that is specialised to particular kinds of interactions or analytes. Particular gases or chemical species may have a greater effect on Zn 3d¹⁰ dominated states, for example. The knowledge regarding the Zn 4s² and O 2p⁴ states in the lowest conduction band is vital for determining the material's conductivity. These orbitals' accompanying changes in the conduction band states may be a sign of interactions with analytes. This is important for sensors whose detection depends on variations in conductivity.

CONCLUSION

Based on the first principles calculation using density functional theory, the adsorption and sensing mechanism of CO gas in Au-ZnO and Pt-ZnO were analysed from this work. This work helped and allowed researchers to understand how changing the composition of doped materials affected the formation energy and band gap. This study demonstrates that the adsorption of CO on Au-ZnO (100% Pt/Au composition) with formation energy of -3743.1074 eV, and Pt-ZnO (100% Pt/Au composition) with formation energy of -3747.4534 eV results in higher adsorption energy and stronger adsorption properties compared to other composition. By comparing Au-

ZnO (100% Pt/Au composition) with Pt-ZnO (100% Pt/Au composition), it can be concluded that Pt-ZnO (100% Pt/Au composition) is preferable as its formation energy is lower than Au-ZnO (100% Pt/Au composition). Moreover, the band gap for Pt-ZnO (100% Pt/Au composition) which is 0.132 eV makes it a good candidate for gas sensor in terms of improving the detection of CO. On top of that, the electrical structure of materials is greatly influenced by intentional doping, as seen in the PDOS analysis. Due to doping-induced fluctuations and Zn 3d¹⁰'s dominance in the highest valence band, the material is extremely sensitive to outside effects. This sensitivity makes sense for sensing applications since it makes it possible to identify environmental changes. Understanding specific orbitals, such as Zn 4s² and O 2p⁴, permits the customization of sensors for specialised interactions or analytes. For sensors that depend on fluctuations in conductivity for detection, knowledge of the material's conductivity especially in the lowest conduction band is crucial. This PDOS study adds important information to the design and optimization of sensors, providing customised solutions for particular sensing needs. Overall, this study indicates that Au or Pt doped ZnO, especially Pt-ZnO with 100% Pt/Au composition, could be a promising candidate for CO gas sensing.

REFERENCES

- [1] S. Wang, J. Cao, Y. Zhao, X. Liu, Y. Guo, J. Chen, W. Wang, R. Zhang, Y. Zhang, X. Liu, and Q. Fu, 2023. Influence of Pt or Au doping on improving the detection of CO by ZnO: A first-principles calculations study, *Chemical Physics*, 570, 111908.
- [2] S. A. Meo, A. A. Abukhalaf, A. A. Alomar, O. M. Alessa, W. Sami, and D. C. Klonoff, 2021. Effect of environmental pollutants PM-2.5, carbon monoxide, and ozone on the incidence and mortality of SARS-COV-2 infection in ten wildfire affected counties in California, *Science of The Total Environment*, 757, 143948.
- [3] S. Mahajan and S. Jagtap, 2020. Metal-oxide semiconductors for carbon monoxide (CO) gas sensing: A review, *Applied Materials Today*, 18, 100483.

- [4] E. Salih and A. I. Ayesh, 2020. CO, CO₂, and SO₂ detection based on functionalized graphene nanoribbons: First principles study, *Physica E: Low-Dimensional Systems and Nanostructures*, 123, 114220.
- [5] Y. Wang, X. Meng, and J. Cao, 2020. Rapid detection of low concentration CO using Pt-loaded ZnO nanosheets, *Journal of Hazardous Materials*, 381, 120944.
- [6] K. Harun, N. A. Salleh, B. Deghfel, M. K. Yaakob, and A. A. Mohamad, 2020. DFT+U calculations for electronic, structural, and optical properties of ZnO wurtzite structure: A review, *Results in Physics*, 16, 102829.
- [7] Y. Vijayakumar, P. Nagaraju, V. Yaragani, S. R. Parne, N. S. Awwad, and M. V. R. Reddy, 2020. Nanostructured Al and Fe co-doped ZnO thin films for enhanced ammonia detection, *Physica B: Condensed Matter*, 581, 411976.
- [8] H. Zhao, Y. Yang, X. Shu, and Y. Wang, 2018. Adsorption of organic molecules on mineral surfaces studied by first-principle calculations: A review, *Advances in Colloid and Interface Science*, 256, 230–241.
- [9] R. Esfandiarpour, F. Zamanian, F. Badalkhani-Khamseh, and M. R. Hosseini, 2022. Carbon dioxide sensor device based on biphenylene nanotube: A density functional theory study, *Computational and Theoretical Chemistry*, 1218, 113939.
- [10] F. Mollaamin and M. Monajjemi, 2023. Doping of Graphene Nanostructure with Iron, Nickel and Zinc as Selective Detector for the Toxic Gas Removal: A Density Functional Theory Study, *Journal of Carbon Research*, 9(1),20, 1-17.
- [11] N. N. Alam, N. A. Malik, M. H. Samat, N. H. Hussin, N. K. Jaafar, A. Radzwan, M. Z. Mohyedin, B. U. Haq, A. M. M. Ali, O. H. Hassan, M. Z. A. Yahya, and M. F. M. Taib, 2021. Underlying mechanism of surface (001) cubic ATiO₃ (A = Pb, Sn) in enhancing thermoelectric

- performance of thin-film application using density functional theory, *Surfaces and Interfaces*, 27, 101524.
- [12] A. M. Pineda-Reyes, M. R. Herrera-Rivera, H. Rojas-Chávez, H. Cruz-Martínez, and D. I. Medina, 2021. Recent advances in ZnO-based carbon monoxide sensors: Role of doping, *Sensors*, 21(13),1-17.
- [13] B. Saruhan, R. L. Fomekong, and S. Nahirniak, 2021. Review: Influences of Semiconductor Metal Oxide Properties on Gas Sensing Characteristics, *Frontiers in Sensors*, 2, 657931.
- [14] V. Kannan, 2020. Adsorption studies on air pollutants using blue phosphorene nanosheet as a chemical sensor – DFT approach, *Computational and Theoretical Chemistry*, 1186, 112910.